# *Articles*

## Defining the Molecular Requirements for the Selective Delivery of Polyamine Conjugates into Cells Containing Active Polyamine Transporters

Chaojie Wang,[†] Jean-Guy Delcros,[‡] Laura Cannon,[§] Fanta Konate,[§] Horacio Carias,[§] John Biggerstaff,[§] Richard Andrew Gardner,[§] and Otto Phanstiel IV*[,§]

*Groupe de Recherche en Therapeutique Anticancéreuse, Faculté de Médecine, 2, Avenue du Professeur Léon Bernard, University of Rennes 1, 35043 Rennes, France, and Department of Chemistry, P.O. Box 162366, University of Central Florida, Orlando, Florida 32816-2366*

*Received May 13, 2003*

Several $N^1$-substituted polyamines containing various spacer units between nitrogen centers were synthesized as their respective HCl salts. The $N^1$-substituents included benzyl, naphthalen-1-ylmethyl, anthracen-9-ylmethyl, and pyren-1-ylmethyl. The polyamine spacer units ranged from generic (4,4-triamine, 4,3-triamine, and diaminooctane) spacers to more exotic [2-(ethoxy)ethanoxy-containing diamine, hydroxylated 4,3-triamine, and cyclohexylene-containing triamine] spacers. Two control compounds were also evaluated: *N*-(anthracen-9-ylmethyl)-butylamine and *N*-(anthracen-9-ylmethyl)-butanediamine. Biological activities in L1210 (murine leukemia), α-difluoromethylornithine (DFMO)-treated L1210, and Chinese hamster ovary (CHO) and its polyamine transport-deficient mutant (CHO-MG) cell lines were investigated via $IC_{50}$ cytotoxicity determinations. $K_i$ values for spermidine uptake were also determined in L1210 cells. Of the series studied, the $N^1$-benzyl-4,4-triamine system **6** had significantly higher $IC_{50}$ values (lower cytotoxicity) in the L1210, CHO, and CHO-MG cell lines. A cellular debenzylation process was observed in L1210 cells with **6** and generated "free" homospermidine. The size of the $N^1$-arylmethyl substituent had direct bearing on the observed cytotoxicity in CHO-MG cells. The $N^1$-naphthalenylmethyl, $N^1$-anthracenylmethyl, and $N^1$-pyrenylmethyl 4,4-triamines had similar toxicity ($IC_{50}$s: ∼0.5 μM) in CHO cells, which have an active polyamine transporter (PAT). However, this series had $IC_{50}$ values of >100 μM, 66.7 μM, and 15.5 μM, respectively, in CHO-MG cells, which are PAT-deficient. The observed lower cytotoxicity in the PAT-deficient CHO-MG cell line supported the premise that the conjugates use PAT for cellular entry. In general, moderate affinities for the polyamine transporter were observed for the *N*-arylmethyl 4,4-triamine series with their L1210 $K_i$ values all near 3 μM. In summary, the 4,4-triamine motif was shown to facilitate entry of polyamine conjugates into cells containing active polyamine transporters.

### Introduction

In vivo the native polyamines **1**−**3** exist as polycations (as the nitrogens are protonated at physiological pH) and are required for cell growth.[1] Their alignment of point charges are recognized by the polyamine transport system and have been shown to facilitate their import.[1−7] Rapidly dividing cells require large amounts of polyamines in order to grow. These can be internally biosynthesized and also imported from exogenous sources. Intracellular polyamine-production constraints in rapidly proliferating cells are thought to be partially offset by scavenging polyamines from extracellular sources.[6] In fact, many tumor types have been shown to contain elevated polyamine levels and an active polyamine transporter (PAT) for importing exogenous polyamines.[6] These range from neuroblastoma, melanoma, human lymphocytic leukemia, colonic, and lung tumor cell lines to murine L1210 cells.[6a] Because of the enhanced cellular need for these amine growth factors and an active transport system for their import, polyamine−drug conjugates can be delivered to cancerous cell types. This is possible due to the broad structural tolerance of the PAT, which allows importation of non-native polyamine constructs.

Previous efforts have shown that specific cell types can be targeted via the molecular recognition events involved during the import of exogenous polyamines.[1−31] Prior work in our laboratories evaluated the cytotoxicity and polyamine transporter (PAT) affinity of conjugates containing branched[1,2] and linear polyamine motifs[3,4] attached to either an anthracene or acridine nucleus.[1,2,14] Indeed, certain linear triamines motifs were identified as excellent vector systems.[3,4] In particular, the 4,4-triamine conjugate **4** (Figure 1, **4**) had 150-fold higher cytotoxicity in CHO cells (which contained an active polyamine transport system) than in a mutant CHO-

* Corresponding author. Phone: (407) 823-5410. Fax: (407) 823-2252. E-mail: ophansti@mail.ucf.edu.
[†] C.W. is a visiting scholar from the Department of Chemistry, Henan University, Kaifeng, 475001, P.R. China.
[‡] University of Rennes 1.
[§] University of Central Florida.

10.1021/jm030223a CCC: $25.00 
Published on Web 10/18/2003

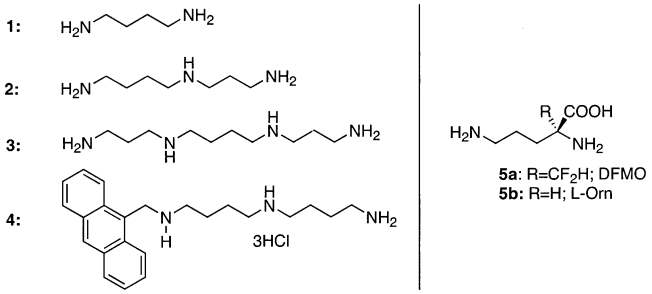


**Figure 1.** Native polyamines putrescine (PUT, **1**), spermidine (SPD, **2**), spermine (SPM, **3**) and anthracenyl-4,4-triamine conjugate **4**, α-difluoromethylornithine, (DFMO, **5a**) and L-ornithine **5b**.

MG cell line, which was PAT-deficient.[3,4,32,33] Therefore, cells which contain an active polyamine transport system were much more sensitive to certain polyamine−anthracene conjugates. The observed differential cytotoxicity formed the basis of a selective chemotherapeutic strategy.

There are several caveats in using polyamines for targeted drug delivery. First, rapidly dividing normal cell types (e.g., bone marrow, intestinal epithelium, and hair follicles) may also be effected by this strategy. Whether polyamine conjugates can discriminate between cancer cell types and these other prolific cell lines remains to be seen. Nevertheless, other authors have observed that transformed cells are more sensitive than normal cells to α-difluoromethylornithine (DFMO, **5a**) pretreatment.[34,35] DFMO is a known ornithine decarboxylase (ODC) inhibitor. As shown in Figure 2, ODC is responsible for putrescine biosynthesis and its inhibition has been shown to increase the uptake of extracellular polyamines.[34] Most pertinent to this study is the observation that when DFMO is dosed in vivo, it increased the uptake of radiolabeled putrescine specifically into tumor cells, and not into other normal tissue, even rapidly growing tissue.[34] This suggests that DFMO treatment may also increase the potency of the present polyamine-conjugates. Second, the $N^1$-component to be delivered in this study (e.g., the arenylmethyl derivatives) are relatively inert, and this conjugation strategy may not be applicable to other drug classes. It is possible that other anticancer agents, which have more "bio-interactive" functional groups, would interact differently with the PAT or other cell surface receptors and diminish the anticipated selectivity. In this report, a relatively inert architecture (e.g., an aryl unit) was used to understand how changes in the $N^1$-substituent and polyamine sequence influenced drug potency and PAT affinity.

The conjugates in this report (**4**[3] and **6**−**15**) are composed of an arene nucleus covalently bound to a polyamine framework. The $N^1$-arenylmethyl unit was selected for alteration due to significant data, which revealed the increased cytotoxicity (lower $IC_{50}$ value) of a $N^1$-anthracenylmethyl conjugate over an *N*-acridinyl analogue in murine leukemia (L1210) cells.[1,2,4,14] In addition, anthracene and the other polycyclic aromatic systems provided a convenient UV "probe" for compound identification and elicit a toxic response from cells upon entry (presumably through DNA coordination).[1−4,36] Therefore, a series of new arene conjugates was synthesized (Figure 3, **6**−**15**) and screened for uptake via the polyamine transporter (PAT).

Their design served two purposes. First, **4** and **6**−**8** provided a homologous series, wherein a variety of arenyl subunits were each attached to the "optimized" 4,4-triamine motif.[3,4] Second, conjugates **9**−**14** provided another series, wherein each member contained the same $N^1$-anthracenylmethyl subunit covalently attached to a modified polyamine vector. By studying how these materials influenced the survival of cells with active and inactive polyamine transport systems, one can relate how conjugate architecture influences cytotoxicity and targeting of specific cell types. In short, by judicious choice of amine substrates (e.g., a synthetic library) and proper biological experiments (e.g., $IC_{50}$, and $K_i$, measurements) in selected cell types (murine leukemia L1210, CHO and CHO-MG cells), a better understanding between transporter affinity, cytotoxicity, and polyamine−drug conjugate structure was obtained.

## Results and Discussion

**Synthesis.** While the terminally bis-alkylated polyamines have yielded diverse biological activity ranging from anticancer to antidiarrheal agents,[5,13] their monosubstituted analogues have limited publications describing their use in vector design.[1−5,14,17,21,23−31] This, in part, may stem from their less direct syntheses, which involve several steps.[3−5,37−39] As shown in Scheme 1, the reductive amination of **16c** was achieved in two steps via in situ generation of the imine **18**. A series of amines (**17a**−**d**) was used to generate the crude imines **18a**−**d**. In general, solvent removal by rotary evaporation at 40−50 °C facilitated the conversion to **18**, which was then reduced to the respective secondary amine using $NaBH_4$ in excellent yield (∼85%). The amines were then acidified with aqueous 4 N HCl to form the target HCl salts: **10** (89%), **11** (81%), **14** (21%), and **15** (58%)[3] (Scheme 1).

Compounds **12** and **13** were prepared using an amino-alkanol strategy, which allowed for control of the amine spacer group.[3,4,37,39] As shown in Scheme 2, the reductive amination of aldehydes **16a**−**d** with 4-amino-1-butanol and $NaBH_4$ provided the substituted amino alcohols **19a**−**d**. The tandem *tert*-butylcarbonylation and tosylation sequence resulted in the intermediates **20a**−**d**, respectively. The tosylates **20a**−**d** were generated as

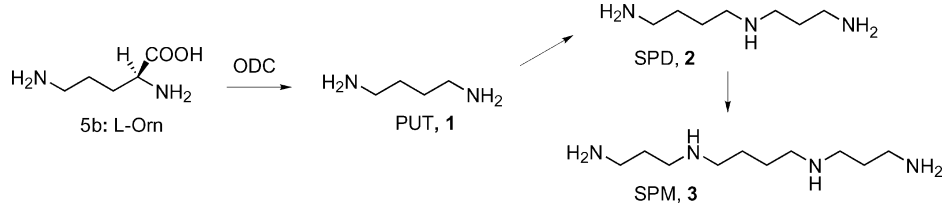


**Figure 2.** Polyamine biosynthetic pathway.

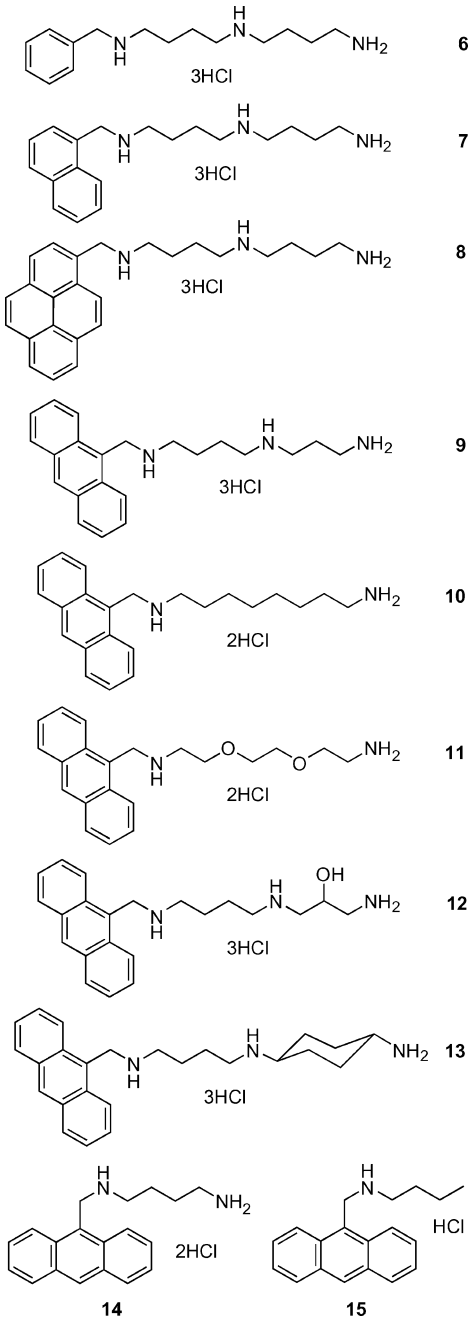


**Figure 3.** Arene−polyamine conjugates.

crude mixtures and used immediately because they were not stable to prolonged storage. Prior experience with these materials revealed that it was not necessary to isolate them. In fact higher yields were obtained, when they were directly consumed in the subsequent step.[3,4] As shown in Scheme 3, crude tosylate **20c** was reacted with either 1,3-diamino-2-hydroxypropane or *trans*-1,4-diaminocyclohexane followed by 4 N HCl to give the respective amino alcohol- and cyclohexyl-containing triamines, **12** and **13** as their HCl salts.

In prior work, tosylate **20c** was converted in two steps to **4**.[3] Using a similar method shown in Scheme 4, the crude tosylates **20a**,**b**,**d** (where **a**−**d** are defined in Scheme 2) were reacted with excess putrescine **1** to form adducts, which were treated with 4 N HCl to give the desired triamines **6**−**8** as their trihydrochloride salts. All the target compounds were purified by washing the

**Scheme 1**

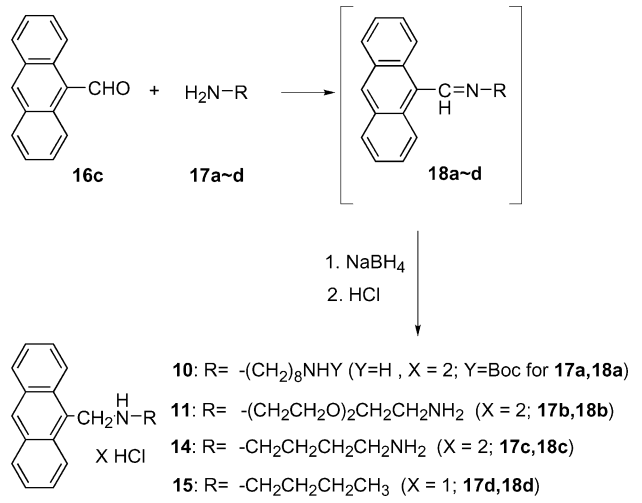


respective HCl salt with absolute ethanol. Compounds **4**, **9**, and **15** were generated in a prior report.[3]

**Biological Evaluation.** Three cell lines were chosen for bioassay. L1210 (mouse leukemia) cells were selected to enable comparisons with the published $IC_{50}$ and $K_i$ values known for a variety of polyamine substrates.[5,29] Chinese hamster ovary (CHO) cells were chosen along with a polyamine transport deficient mutant cell line (CHO-MG) in order to comment on selective transport via the PAT.[3,4,14]

Inhibition of ODC by DFMO (**5a**) depletes intracellular polyamine pools and leads to a significant increase in polyamine uptake.[34,35] Therefore, cells, which are treated with DFMO, should be more susceptible to the polyamine-vectored conjugates and should provide lower $IC_{50}$ values.[3,4,6,14] $IC_{50}$ values in L1210 cells with and without DFMO-treatment were determined. Conjugates, which selectively target the PAT, should provide L1210/(L1210+DFMO) $IC_{50}$ ratios greater than 1. In fact, prior work in L1210 cells revealed an approximate doubling of potency of certain triamine derivatives (50% reduction in $IC_{50}$ value) with DFMO treatment.

As shown in Table 1, a range of cytotoxicities was observed, with **4** being the most cytotoxic and the *N*-benzyl derivative **6** being the least efficacious. As expected the controls **14** and **15** gave relatively low cytotoxicity (and $IC_{50}$ ratios $<1$) in both normal and DFMO-treated L1210 cells (Table 1). Within the homologous series (**4** and **6**−**8**), the $N^1$-naphthylmethyl **7**, $N^1$-anthracenylmethyl **4**, and $N^1$-pyrenylmethyl **8** derivatives had similar cytotoxicity both in the presence and absence of DFMO. The dramatic reduction in cytotoxicity for **6** was explained by the observation of homospermidine (i.e., $H_2N(CH_2)_4NH(CH_2)_4NH_2$) within cells treated with **6** (data not shown).

When DFMO-treated cells are depleted of putrescine and spermidine, homospermidine can support cell growth.[40a] A catabolic process whereby the *N*-benzyl group was cleaved via cellular metabolism was observed by the detection of homospermidine in the HPLC analysis of perchloric acid extracts of cells treated with **6** using OPA postcolumn derivatization.[40b] Alternatively, the detection of free homospermidine was also facilitated by conversion to its dansyl derivative (see

**Scheme 2**

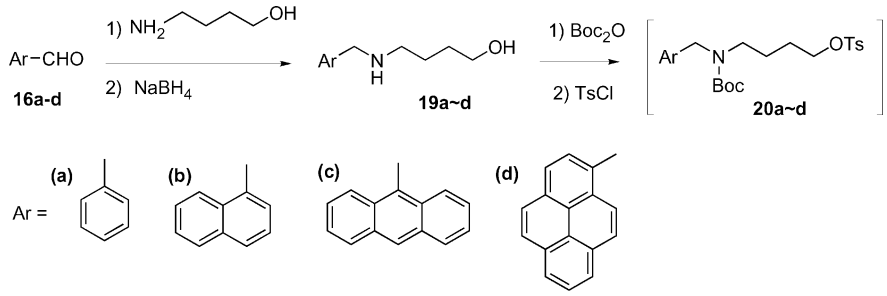


**Scheme 3**

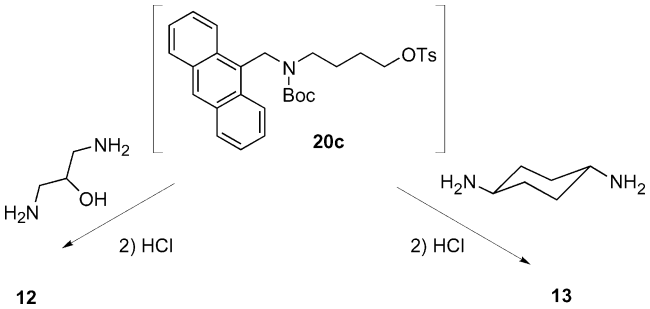


**Scheme 4**

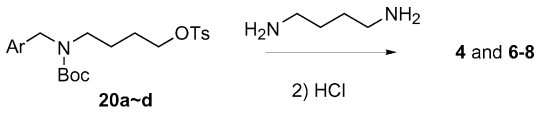


Ar= a) phenyl, b) naphthyl, c) anthracenyl, and d) pyrenyl

Experimental Section) and measured via mass spectrometry.[40c,d] Only trace quantities of homospermidine were detected in L1210 cells treated with **7** and none with **4** or **8**.

Similar findings were reported by Delcros and coworkers, who demonstrated the catabolization of *N*-benzylspermidine ($PhCH_2NH(CH_2)_3NH(CH_2)_4NH_2$) to form free spermidine **2**.[40d] Other N-dealkylations have been reported by Bergeron et al. in their study of $N^1$-propylpolyamines.[5] For example, the $N^1$,$N^7$-dipropyl-3,3-triamine and $N^1$,$N^8$-dipropyl-4,4-triamine derivatives were converted to their corresponding monopropyl derivatives in 40% and 12%, respectively. The current findings with **6**, **7**, **4**, and **8** suggest a possible size limitation for the $N^1$ dealkylating enzyme in terms of its inability to process the larger $N^1$-substituents.

Previous studies revealed the similar $IC_{50}$ values of the Ant-(4,4)-triamine **4** and Ant-(4,3)-triamine **9** derivatives in L1210 cells.[3] Comparison of **9**−**12** provided additional insights. Exchange of the internal nitrogen with a $CH_2$ group (**10**) or hydroxylation of the methylene chain (**12**) gave higher $IC_{50}$ values than found with the parent system **9**. Introduction of the polyether chain (**11**) in lieu of the methylene chain present in **10** resulted in a conjugate with lower toxicity and low affinity for the PAT ($K_i$ value: 90 $\mu$M). Not surprisingly, the cyclohexyl derivative **13** had a similar profile as its parent **4** in L1210 cells (with and without DFMO treatment). Overall, DFMO treatment gave little to no enhancement of cytotoxicity for most systems studied with the exception of **4** and **9**.

The $K_i$ value is a measure of the affinity of the polyamine conjugate for the polyamine transporter and was determined in a competitive assay with radiolabeled spermidine.[3,4,14,41] It should be noted that there are numerous modes of entry for polyamines into cells and that each mode may have a different structure−activity relationship with our synthetic ligands. At present, we were unable to discreetly measure each of these modes of import. Therefore, the listed $K_i$ values (Table 1) reveal the overall transporter affinity of each synthetic conjugate when all these uptake modes are active in L1210 cells. These collective polyamine uptake modes will be referred to as the "polyamine transporter" or PAT.

The affinities of substituted amine conjugates (**4, 6**−**15**) for the PAT in L1210 cells (i.e., $K_i$ values) are listed in Table 1. As expected the controls **14** and **15** gave high $K_i$ values (low PAT affinity) and as mentioned above no enhancement of toxicity with DFMO treatment. This is consistent with earlier work which showed that the innate affinity for the L1210 polyamine transporter decreased with decreasing number of nitrogen centers.[4] In other words, tetraamines had higher PAT affinity than triamines, triamines had higher affinity than diamines, etc. Several of the triamine derivatives (**4**, **6**−**9**, **13**) demonstrated moderate affinity for PAT ($K_i$ values $< 6.2$ $\mu$M). This feature was shown to be an important parameter for facile import via the polyamine transporter. Prior studies had shown that high-affinity PAT ligands (like *N*-anthracenylmethyl-tetraamine conjugates) were not as potent cytotoxic agents as conjugates with moderate PAT affinity (e.g., related triamines).[4]

Why are some analogues more cytotoxic than others? One interpretation is that **4** is simply intrinsically more toxic to the cell than the related controls **14** and **15**. This would assume that the polyamine architecture itself is toxic to the cell and that different polyamine scaffolds will have different cytotoxicities. Previous work, however, demonstrated that unsubstituted polyamines (i.e. the 4,4-triamine) were not toxic to cells.[3,4,40a] A more intriguing answer may lie in how efficiently these materials recognize the PAT cell-surface receptor and are transferred into the cell (or to their cellular target). In light of the differential PAT affinities ($K_i$ values) observed with the unsubstituted polyamines,[4] the latter premise seems reasonable. In other words, the polyamine "message" appears to be required for PAT recognition. Changes in this message may also lead to differential import rates ($V_{max}$).[4]

An assessment of the conjugates' ability to target the PAT was conducted in two Chinese hamster ovary (CHO) cell lines. The CHO-MG cell line is a polyamine-transport deficient mutant, which was isolated for growth resistance to MGBG, methylglyoxalbis(guanyl-

**Table 1.** Biological Evaluation of Polyamine Derivatives in L1210 Cells[a]

| compd (tether) | L1210 $IC_{50}$ in $\mu$M | L1210+DFMO $IC_{50}$ in $\mu$M | L1210/(L1210+DFMO) $IC_{50}$ ratio[a] | $K_i$ values ($\mu$M) L1210 cells |
|---|---|---|---|---|
| **4:** Ant (4,4) | 0.30 (±0.04) | 0.15 (± 0.10) | 2 | 1.8 (±0.1) |
| **6:** benzyl (4,4) | 36.3 (± 8.4) | 421.0 (± 27.1) | 0.1 | 4.5 (± 0.8) |
| **7:** naphthyl (4,4) | 0.50 (±0.03) | 0.43 (± 0.02) | 1.1 | 3.8 (±0.5) |
| **8:** pyrenyl (4,4) | 0.40 (±0.02) | 0.36 (± 0.06) | 1.1 | 2.9 (±0.3) |
| **9**: Ant (4,3) | 0.4 (±0.1) | 0.20 (± 0.02) | 2 | 6.2 (±0.6) |
| **10:** Ant-(octylene) | 3.00 (± 0.07) | 4.60 (± 0.12) | 0.7 | 13.3 (±1.5) |
| **11:** Ant-(diethoxy) | 11.30 (±0.37) | 17.00 (± 0.61) | 0.7 | 90.0 (±4.6) |
| **12:** Ant- (4,3-hydroxyamino) | 1.50 (±0.08) | 2.30 (± 0.29) | 0.7 | 12.5 (±1.2) |
| **13:** Ant-(cyclohexyl) | 1.00 (±0.16) | 0.7 (± 0.1) | 1.4 | 3.8 (±0.9) |
| **14:** Ant-(butanediamine) | 6.30 (±0.26) | 9.78 (± 0.42) | 0.7 | 32.2 (±4.3) |
| **15:** Ant (*N*-butyl) | 14.6 (±0.1) | 21.9 (±3.6) | 0.7 | 62.3 (±4.2) |

[a] Note: the individual L1210 $IC_{50}$ values are listed in $\mu$M and the ratio is dimensionless.

**Table 2.** Biological Evaluation of Polyamine Derivatives in the CHO-MG and CHO Cell Lines

| compound (tether) | CHO-MG $IC_{50}$ in $\mu$M | CHO $IC_{50}$ in $\mu$M | (CHO-MG/CHO) $IC_{50}$ ratio |
|---|---|---|---|
| **4:** Ant (4,4) | 66.7 (± 4.1) | 0.45 (± 0.10) | 148 |
| **6:** benzyl (4,4) | >1000 | >1000 | NA |
| **7:** naphthyl (4,4) | >100 | 0.6 (±0.2) | >164 |
| **8:** pyrenyl (4,4) | 15.5 (±2.4) | 0.46 (±0.05) | 34 |
| **9**: Ant (4,3) | 9.5 (±1.1) | 0.4 (± 0.1) | 24 |
| **10:** Ant-(octylene) | 4.9 (±0.1) | 4.9 (± 0.2) | 1 |
| **11:** Ant-(diethoxy) | 15.9 (±1.5) | 12.6 (± 0.6) | 1.3 |
| **12:** Ant- (4,3-hydroxyamino) | 9.5 (±0.8) | 9.1 (± 0.4) | 1 |
| **13:** Ant-(cyclohexyl) | 17.4 (±2.8) | 2.5 (± 0.5) | 7 |
| **14:** Ant-(butanediamine) | 7.6 (±0.4) | 7.7 (± 0.5) | 1 |
| **15:** Ant (*N*-butyl) | 11.2 (±2.3) | 10.5 (± 2.0) | 1.1 |

hydrazone), using a single-step selection after mutagenesis with ethyl methane sulfonate.[32] MGBG is a known substrate for PAT.[32] For the purposes of this study, the CHO-MG cell line represented cells with limited polyamine transporter activity and provided a measure of delivery independent of the PAT. In contrast, the parent CHO cell line represented cell types with active polyamine transport.[32,33] Comparison of conjugate toxicity in these two lines provided an important screen to detect conjugate delivery via the PAT. For example, a conjugate with high utilization of the transporter would be very toxic to CHO cells, but less so to CHO-MG cells.[3,4,14]

As shown in Table 2, the controls **14** and **15** gave the same toxicity in both CHO and CHO-MG cells (CHO-MG/CHO $IC_{50}$ ratios near 1). The conjugates **10**−**12** also gave similar $IC_{50}$ values in both CHO cell lines. As expected, this suggested that neither of these conjugates were using the PAT to gain access to the cell and is consistent with their corresponding low PAT affinity (as observed in L1210 cells, with the respective $K_i$ values >12.5 $\mu$M). The *N*-benzyl derivative **6** was nontoxic to both CHO cell lines. The remaining members of the $N^1$-aryl homologous series, *N*-naphthylmethyl **7**, *N*-anthracenylmethyl **4**, and *N*-pyrenylmethyl **8**, gave similar cytotoxicities in CHO cells ($IC_{50}$s ~ 0.5 $\mu$M). In general, the more hydrophobic the conjugate (e.g., **8**), the more cytotoxic it was to the PAT-deficient CHO-MG cells. For example, the pyrene-containing conjugate **8** (ratio: 34) gave a lower (CHO-MG/CHO) $IC_{50}$ ratio than **4** (ratio: 148) and **7** (ratio: >164). In addition, the cyclohexyl derivative **13** is more hydrophobic than **4** and was more toxic (than **4**) in CHO-MG cells. In fact **13** had similar cytotoxicity as **8** in this cell line. This effect was likely due to differential transport, wherein the hydrophobic ligand accessed the cell via a non-PAT-mediated pathway.

Evaluation of the triamine series in the two CHO cell lines revealed striking preferences by certain polyamine architectures for the PAT. Prior findings suggested the 4,4-triamine **4** as an excellent vector as its anthracene conjugate displayed a nearly 150-fold higher toxicity in CHO cells over the CHO-MG cell line.[13] However, this study revealed that the selective targeting of cells with active polyamine transporters can be further enhanced via the smaller, less hydrophobic naphthylmethyl unit in **7**. Of the series tested, the naphthylmethyl triamine **7** gave the best selectivity profile. In short, **7** had relatively low toxicity in cells with low PAT activity and high toxicity in cells with high polyamine transport activity. Moreover, our findings reiterate that CHO and CHO-MG $IC_{50}$ comparisons are an excellent way to rank polyamine vectors and their transport.[14] As before[3], the cytotoxicity of the triamines in the CHO lines correlated nicely with the L1210 $IC_{50}$ and $K_i$ results.

A priori one may have expected that polyamines with bulky N-substituents would be poor ligands for the polyamine transporter. However, earlier comparisons suggested that the bulky *N*-(arylmethyl) substituent actually enhances the PAT binding affinity and cytotoxicity of the polyamine conjugate in vitro.[4] Although aromatic substituents seem to impart higher affinity for cell-surface receptors, there are limitations. As seen with **8** if the arene unit is too hydrophobic then the selectivity for the polyamine transporter is diminished (Table 2). Using deconvolution microscopy, conjugates such as **4** with high cytotoxicity had a high qualitative rate of import. By comparison a related anthracene tetraamine conjugate with lower cytotoxicity was less internalized during the same time period. These preliminary findings suggested that the differential cytotoxicities could be explained by different rates of transport into the cell.[4] Collectively, these observations further support the ability of certain cell types to

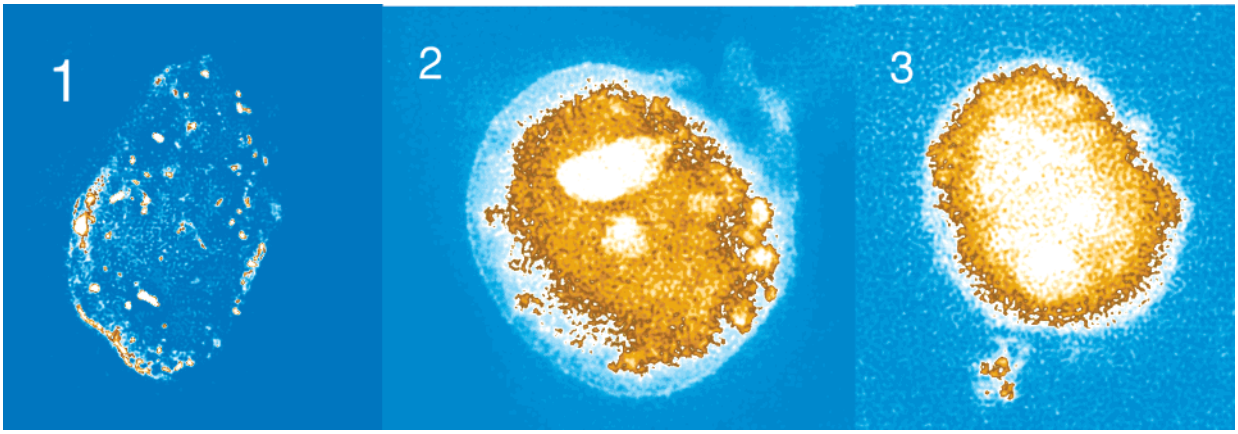


**Figure 4.** Deconvolution microscopy images of detached A375 cells treated with **4** (Panels 1−3). Panel 1 (3 min),[4] Panel 2 (10 min), and Panel 3 (60 min) represent cells incubated with **4**, for the respective time period, at 10 $\mu$M, then washed with buffer and fixed with paraformaldehyde.

recognize the conjugates via their polyamine motifs and $N^1$-substituents.

To further address this issue, we conducted a time-course microscopy study to observe the delivery profile of **4** into A375 melanoma cells. Melanoma cells were chosen due to their large size and susceptibility to polyamine analogues.[4,6a] A375 cells were incubated with conjugate **4** (at 10 $\mu$M) for 3, 10, and 60 min time intervals. A series of optical "slices" of the resultant cells were obtained, and one slice was chosen to best represent the sample overall. The UV spectra of the anthracene conjugates suggest a consistent $\lambda_{max}$ near 364 nm and an emission maxima near 417 nm. Therefore, the anthracene component was easily tracked via its diagnostic fluorescence properties and selected images from the time-course study are shown in white/gold in Figure 4. The relative levels of fluorescence inside the cell (at early and late times) confirmed the expected time-dependent transport phenomenon. Panel 1 in Figure 4 revealed that the triamine conjugate **4** rapidly accessed the cell as evidenced by the large number of fluorescent vesicles inside the cell after a three minute exposure of cells to **4**.[4]

The samples were washed before they were fixed with paraformaldehyde and imaged by deconvolution microscopy. Prior studies showed that both the surface-bound and unbound triamine were efficiently washed away from the cell surface in the workup step.[4] The limited amount of triamine bound to the cell surface is consistent with the lower binding affinity of this probe to PAT (Table 2) and presumably other membrane receptors.[4] Conversely, high affinity tetraamine ligands (e.g., L1210 $K_i$ values in the nM range) were shown to bind irreversibly to the membrane and gave large amounts of conjugate still bound to the cell surface after a buffer wash.[4] The lower cytotoxicity of the higher affinity tetraamine systems was rationalized by their indiscriminate binding to numerous cell surface receptors which likely result in dramatic changes in membrane fluidity and transport (e.g., endocytosis).[4]

The findings were also consistent with a model proposed by Cullis and Poulin.[6a,30,43] First, polyamines bind to a surface receptor, which results in membrane envagination (endocytosis) to create polyamine-rich vesicles inside the cell. The derivative may then be exported out of this vesicle to a particular cellular compartment via a cationic symporter.[30] Indeed, panel 1 in Figure 4, seems to have captured this endocytosis event in action. Using the same model, to exit the vesicle (via the putative cationic symporter), the conjugate must dissociate from its vesicular PAT receptor. Since triamines have moderate binding affinities they should be able to dissociate from the internalized PAT receptor to exert their toxic effect. Panel 2 (at 10 min) revealed an increase in the number and size of the internalized vesicles. Inspection of Panel 3 (at 60 min) in Figure 4 suggests that at latter times the conjugate **4** has escaped the initially formed vesicles seen in Panel 1 and is delivered throughout the cell. To the best of our knowledge, this is the first time-course study of a polyamine import process using a fluorescent, bioactive-marker.

A polyamine transporter gene has not yet been identified in mammalian cells. In fact, little is known about the structural aspects of the polyamine transporter (PAT) itself. Proteoglycans may play a role in polyamine transport.[44] Proteoglycans are composed of glycosaminoglycan chains covalently linked to protein and expression of cell-surface proteoglycans are required for the binding of many extracellular substrates.[44c] Indeed, inhibition of polyamine biosynthesis with DFMO resulted in an increase of cell-associated proteoglycans exhibiting higher affinity for spermine in a human lung fibroblast study.[44c] The data indicated a specific role for heparan sulfate proteoglycans (HSPG) in the uptake of spermine by fibroblasts. These provocative results suggest that proteoglycan-mediated polyamine transport may play an important role in future drug delivery strategies.[45,46] The current report also provides new fluorescent probes needed to evaluate these interesting new pathways.

In summary, the polyamine transporter is capable of distinguishing between systems, which have the same overall length, but a different separation of point charges and $N^1$-substituents.[3,4,26−29] The current study identified hydrophobicity (and possible size) limitations of the appended arenyl unit, which influence the selectivity profile of the polyamine conjugate. Conjugates containing the presence of a 4,4-triamine sequence, moderate PAT affinity ($K_i$ values near 1 $\mu$M), moderate hydrophobicity (e.g., **4** or **7**), and high (CHO-MG/CHO) $IC_{50}$ ratios were shown to target cells via the PAT pathway with high specificity.

## Conclusions

A series of $N^1$-substituted polyamines containing different spacer units between nitrogen centers was synthesized. DFMO-treated L1210 cells were not overly sensitive to most of the conjugates evaluated with the exception of **4** and **9.** A survey of different polyamine vectors revealed that the respective 4,4-triamine system had high selectivity for CHO cells containing active polyamine transporters. Optimal use of this transporter seems to require a balance between PAT binding affinity, conjugate internalization via vesicles, and escape to the cellular target.

In summary, selective vector motifs were identified, which enable cellular entry via the polyamine transporter (PAT). Since many cancer cell lines have high PAT activity, especially when dosed with DFMO,[34] these results further illustrate a novel anticancer strategy.

## Experimental Section

**Materials.** Silica gel (32−63 $\mu$m) and chemical reagents were purchased from commercial sources and used without further purification. All solvents were distilled prior to use. $^1$H and $^{13}$C NMR spectra were recorded at 300 and 75 MHz, respectively. TLC solvent systems are based on volume %, and $NH_4OH$ refers to concentrated aqueous $NH_4OH$. Elemental analyses were performed by Atlantic Microlabs (Norcross, GA). High-resolution mass spectrometry was performed by Dr. David Powell at the University of Florida Mass Spectrometry facility.

**Biological Studies.** Murine leukemia cells (L1210), CHO, and CHO-MG cells were grown in RPMI medium (Eurobio, Les Ulis, France) supplemented with 10% fetal calf serum, 2 mM glutamine (2 mM), penicillin (100U/mL), and streptomycin (50 $\mu$g/mL) (BioMerieux, Marcyl'Etoile, France). L-Proline (2 $\mu$g/mL) was added to the culture medium for CHO-MG cells. Cells were grown at 37 °C under a humidified 5% $CO_2$ atmosphere. Aminoguanidine (2 mM) was added to the culture medium to prevent oxidation of the drugs by the enzyme (bovine serum amine oxidase) present in calf serum. Trypan blue staining was used to determine cell viability before the initiation of a cytotoxicity experiment. Typically, samples contain less than 5% trypan blue positive cells (dead). For example, L1210 cells in early to mid log-phase were used.

**$IC_{50}$ Determinations.** Cell growth was assayed in sterile 96-well microtiter plates (Becton-Dickinson, Oxnard, CA). L1210 cells were seeded at $5 \times 10^4$ cells/mL of medium (100 $\mu$L/well). Single CHO and CHO-MG cells, harvested by trypsinization were plated at $2 \times 10^3$ cells/mL. Drug solutions (5 $\mu$L per well) of appropriate concentration were added at the time of seeding for L1210 cells and after an overnight incubation for CHO and CHO-MG cells. In some experiments DFMO (5 mM) was added in the culture medium at the time of drug addition. After exposure to the drug for 48 h, cell growth was determined by measuring formazan formation from 3-(4,5-dimethylthiazol-2-yl)-2,5-diphenyltetrazolium using a Titertek Multiskan MCC/340 microplate reader (Labsystems, Cergy-Pontoise, France) for absorbance (540 nm) measurements.[47]

**$K_i$ Procedure.** The ability of the conjugates to interact with the polyamine transport system were determined by measuring competition by the conjugates against radiolabeled spermidine uptake in L1210 cells. This procedure was used to obtain the data listed in Table 1. Initially, the $K_m$ value of spermidine transport was determined in a reaction volume of 600 $\mu$L of Hanks's balanced salt solution (HBSS) containing $3 \times 10^6$ cells/mL in the presence of 0.5, 1, 2, 4, 6, and 8 $\mu$M [$^{14}$C]-spermidine. The cell suspensions were incubated at 37 °C for 10 min. The reaction was stopped by adding 3 mL ice-cold phosphate-buffered saline (PBS). The tubes were centrifuged, and the supernatant was removed. The cell pellets were then washed twice with ice-cold PBS, and the supernatant was removed. The pellet was broken by sonication in 500 $\mu$L of 0.1% Triton in distilled water. Two hundred microliters of the cell lysate was transferred in a 5 mL scintillation vial containing 3 mL of Pico-Fluor15. The respective radioactivity of each sample was measured using a scintillation counter. The $K_m$ value of spermidine transport was determined by Lineweaver−Burke analysis as described.[48]

The ability of conjugates to compete for [$^{14}$C]spermidine uptake were determined in L1210 cells by a 10-min uptake assay in the presence of increasing concentrations of competitor, using 1 $\mu$M [$^{14}$C]spermidine as substrate. $K_i$ values for inhibition of spermidine uptake were determined using the Cheng−Prusoff equation[41] from the $IC_{50}$ value derived by iterative curve fitting of the sigmoidal equation describing the velocity of spermidine uptake in the presence of the respective competitor.[43,49] Cell lines (murine leukemic L1210 cells) were grown and maintained according to established procedures.[7,42] Cells were washed twice in HBSS prior to the transport assay.

**Deconvolution Microscopy.** The microscope system included an Applied Precision (Issaquah, WA) Deltavision system equipped with a Nikon Eclipse TE200 inverted microscope. Image deconvolution was performed using Applied Precision SoftWorX software. Detached melanoma A375 cells[3] were incubated with **4** (10 $\mu$M) at 37 °C for the respective time interval in a culture medium containing 10% fetal bovine serum in RPMI-1640 media containing phenol red and an antibiotic cocktail. The cells were then washed with fresh phosphate-buffered saline (PBS) and centrifuged, and the supernatant was removed. The cellular pellet was resuspended in fresh PBS, fixed with paraformaldehyde, and placed onto a microscope slide and imaged by the deconvolution microscope. This technique provides an image of the entire cell by using software to overlay a series of planar images (or slices) to give a stacked translucent view of the entire cell. The lightest regions in Figure 4 contain the highest concentration of the fluorescent conjugate.

**General Procedure for Imine Formation**. To a stirred solution of amine derivative (12 mmol) in 25% MeOH/$CH_2Cl_2$ (10 mL), was added a solution of 9-anthraldehyde (10 mmol) in 25% MeOH/$CH_2Cl_2$ (10 mL) under $N_2$. The mixture was stirred at room-temperature overnight until the imine formation was complete (monitored by TLC). The solvent was evaporated under vacuum to give the crude imine **18** as a bright green solid, which was used for reduction without further purification.

**General Procedure for the Reduction of Imines**. $NaBH_4$ (30 mmol) was added in small portions to the solution of crude imine in 1:1 $CH_3OH$ :$CH_2Cl_2$ (20 mL) at 0 °C. The mixture was stirred at room-temperature overnight, then concentrated under vacuum. The residue was dissolved in $CH_2Cl_2$ (50 mL) and washed three times with 50 mL of aqueous $Na_2CO_3$ (pH = 10). The organic layer was separated, dried over anhydrous $Na_2SO_4$, filtered, and concentrated under vacuum. The residue was purified by flash chromatography on silica gel to provide the secondary amines, which were immediately converted to their HCl salts (see General Procedure for the HCl Salt Formation).

**General Procedure for N-Boc Protection and Tosylation.** Note: During the synthesis of starting $N^1$-BOC diaminooctane (**17a**) the molar ratio of 1,8-diaminooctane to $Boc_2O$ was 3:1. The other BOC reactions were performed in the following molar ratios.

**N-Boc Introduction**. As an example, a solution of the respective secondary amine **19** (5 mmol) in triethylamine−methanol (1:9 V/V, 20 mL) was stirred at 0 °C for 10 min, then a solution of di-*tert* -butyl dicarbonate (7.5 mmol) in methanol (5 mL) was added dropwise over 10 min. The mixture was stirred for an additional 1 h at 0 °C. The temperature was allowed to gradually rise to room temperature, and the reaction was stirred overnight. The mixture was evaporated under reduced pressure. The residue was dissolved in $CH_2Cl_2$ and washed with deionized water several times. The organic layer was separated, dried with anhydrous $Na_2SO_4$, filtered, and concentrated. The residue could be purified by flash

column chromatography on silica gel (to give ≥84% yield)[3] or be used in the next step without further purification.

***O*-Tosylation (Preparation of 20).** A solution of the N-Boc protected alcohol (5 mmol) in dry pyridine (20 mL) was stirred at 0 °C for 10 min. *p*-Toluenesulfonyl chloride (TsCl, 7.5 mmol) was added in small portions over 30 min. The mixture was stirred for an additional 1 h at 0 °C, then the reaction flask was placed in a refrigerator (0−5 °C) overnight. The mixture was poured into 200 mL of ice−water, and a viscous liquid typically precipitated. After the upper water layer was decanted, the remaining viscous liquid was dissolved in methylene chloride and washed with deionized water several times. These steps avoided an emulsion during the extraction workup. The organic layer was separated, dried with anhydrous $Na_2SO_4$, filtered, and concentrated. The residue could be purified by flash column chromatography on silica gel (to give 50−88% yields)[3] or be used in the next step without further purification.[3,4]

**General Procedure for the Substitution of the Tosylated Compounds with Different Diamines.** The crude tosylate **20** (1 mmol) and the respective diamine (5 mmol) were dissolved in acetonitrile (10 mL) and stirred at 75 °C under $N_2$ overnight. After disappearance of the tosylate was confirmed by TLC, the solution was concentrated under reduced pressure. The residue was dissolved in $CH_2Cl_2$ (20 mL) and washed three times with saturated aqueous sodium carbonate. The organic layer was separated, dried with anhydrous sodium sulfate, filtered, and concentrated under vacuum. The residue was purified by flash column chromatography on silica gel. The purified products were isolated in good yields (60−75%) and converted to their HCl salts as described below.

**General Procedure for the HCl Salt Formation (Preparation of 4 and 6−15).** The respective amine or N-Boc protected amine (0.5 mmol) was dissolved in EtOH (5 mL) and stirred at 0 °C for 10 min. 4 N HCl (8 mL) was added dropwise at 0 °C. The reaction mixture was stirred at room-temperature overnight. The solution was concentrated under reduced pressure below 40 °C and typically gave a bright yellow solid as a precipitate. The solids were washed several times with absolute ethanol and dried under vacuum to give the pure target compounds (**4** and **6**−**15**). The yields were typically >70%.

**Note**: Compounds **4**, **9**, and **15** were synthesized in a previous report.[3]

***N*-(4-Amino-butyl)-*N*′-benzene-1-ylmethyl-butane-1,4-diamine Trihydrochloride (6).** White solid; yield 73%. $^1$H NMR (300 MHz, DMSO+$D_2O$): $\delta$ 7.47 (br s, 2H), 7.41 (br s, 3H), 4.09 (s, 2H), 2.88 (br s, 6H), 2.78 (br s, 2H), 1.63 (br s, 8H). $^{13}$C NMR ($D_2O$): 130.7, 129.9 (2C), 129.8, 129.4 (2C), 51.3, 47.13, 47.07, 46.5, 39.0, 24.2, 23.1, 23.0 (2C); HRMS (FAB): calcd for $C_{15}H_{28}N_3$ (M + H − 3HCl)$^+$: 250.2283; found: 250.2268. Anal. ($C_{15}H_{30}Cl_3N_3$) C, H, N.

***N*-(4-Amino-butyl)-*N*′-naphthalen-1-ylmethyl-butane-1,4-diamine Trihydrochloride (7).** White solid; yield 80%. $^1$H NMR (300 MHz, $D_2O$): $\delta$ 8.03 (brs, 1H), 7.96 (brs, 2H), 7.59 (brs, 2H), 7.53 (brs, 1H), 7.51 (brs, 1H), 4.68 (s, 2H), 3.14 (t, 2H), 2.99 (m, 6H), 1.67 (brs, 8). $^{13}$C NMR ($D_2O$): 132.9, 130.2, 129.9, 128.8, 128.5, 126.8, 126.0, 125.8, 125.0, 121.9, 47.4, 46.5, 46.4, 46.3, 38.4, 23.5, 22.5, 22.4 (2C); HRMS(FAB): calcd for $C_{19}H_{30}N_3$ (M + H − 3HCl)$^+$: 300.2440; found: 300.2431. Anal. ($C_{19}H_{32}Cl_3N_3$·0.57$H_2O$) C, H, N.

***N*-(4-Amino-butyl)-*N*′-pyren-1-ylmethyl-butane-1,4-diamine Trihydrochloride (8).** White solid; yield 94%. $^1$H NMR (300 MHz, $D_2O$): $\delta$ 8.1∼7.6 (m, 9H), 4.46 (s, 2H), 3.04 (m, 2H), 2.92 (m, 6H), 1.63 (br s, 8H). $^{13}$C NMR ($D_2O$): $\delta$ 131.3, 130.4, 129.7, 128.4, 128.2, 127.9, 126.9, 126.3, 125.7, 125.6, 124.53, 124.51, 123.1, 122.9, 122.5, 120.9, 47.9, 47.0, 46.9, 46.6, 39.0, 24.1, 23.0, 22.9 (2C). HRMS (FAB): calcd for $C_{25}H_{31}N_3$ (M + H − 3HCl)$^+$: 374.2596; found: 374.2594. Anal. ($C_{25}H_{34}Cl_3N_3$·1.2$H_2O$) C, H, N.

***N*$^1$-Anthracen-9-ylmethyl-octane-1,8-diamine Dihydrochloride (10).** Yellow solid; yield 89%; $^1$H NMR (300 MHz, $CD_3OD$) $\delta$ 8.69 (s, 1H), 8.40 (d, 2H), 8.15 (d, 2H), 7.70 (t, 2H), 7.59 (t, 2H), 5.32 (s, 2H), 3.30 (br s, 2H), 2.92 (t 2H), 1.82 (m, 2H), 1.63 (m, 2H), 1.42 (br s, 8H); $^{13}$C NMR ($D_2O$): $\delta$ 130.6, 130.3, 130.0, 129.4, 127.6, 125.5, 122.4, 120.5, 47.8, 42.3, 39.7, 28.2, 28.1, 26.9, 25.9, 25.7, 25.4; HRMS (FAB) *m*/*z* calcd for $C_{23}H_{31}N_2$ (M + H − 2HCl)$^+$: 335.2487; found: 335.2489. Anal. ($C_{23}H_{32}Cl_2N_2$) C, H, N.

**{8-[(Anthracen-9-ylmethyl)-amino]-octyl}-carbamic acid *tert*-butyl Ester (10a).** The secondary amine precursor to **10** was also isolated after $NaBH_4$ reduction. **10a**: yellow viscous liquid; yield 84%; $R_f$ = 0.24, methanol/chloroform, 1:99; $^1$H NMR (300 MHz, $CDCl_3$) $\delta$ 8.40 (s, 1H), 8.36 (d, 2H), 8.00 (d, 2H), 7.53 (t, 2H), 7.46 (t, 2H), 4.72 (s, 2H), 4.50 (br s, 1H, BocNH), 3.08 (m, 2H), 2.84 (t, 2H), 1.60 (m, 2H), 1.42 (br s, 10H), 1.28 (br s, 9H); $^{13}$C NMR: $\delta$ 155.7, 131.6, 131.3, 130.0, 128.9, 126.9, 125.9, 124.7, 123.9, 78.9, 50.5, 45.7, 40.6, 30.0 (2C), 29.4, 29.2, 28.4, 27.3, 26.7; HRMS (FAB) *m*/*z* calcd for $C_{28}H_{39}N_2O_2$ (M + H)$^+$: 435.3012; found: 435.3048. Anal. ($C_{28}H_{38}N_2O_2$·0.15$H_2O$) C, H, N.

**2-(2-{2-[(Anthracen-9-ylmethyl)-amino]-ethoxy}-ethoxy)-ethylamine Dihydrochloride (11).** Bright yellow solid; yield 81%; $^1$H NMR (300 MHz, DMSO-$d_6$ +$D_2O$) $\delta$ 8.80 (s, 1H), 8.40 (d, 2H), 8.20 (d, 2H), 7.68 (t, 2H), 7.60 (t, 2H), 5.24 (s, 2H), 3.82 (t, 2H), 3.66 (m, 4H), 3.60 (t, 2H), 3.40 (t, 2H), 2.96 (t, 2H); $^{13}$C NMR($D_2O$): $\delta$ 130.8, 130.5, 130.1, 129.5, 127.7, 125.6, 122.5, 120.5, 69.8 (2C), 66.6, 65.1, 47.0, 42.5, 39.2. HRMS (FAB) *m*/*z* calcd for: $C_{21}H_{27}N_2O_2$ (M + H-2HCl)$^+$: 339.2073; found: 339.2074. Anal. ($C_{21}H_{28}Cl_2N_2O_2$) C, H, N.

**1-Amino-3-{4-[(anthracen-9-ylmethyl)-amino]-butyl-amino}-propan-2-ol Trihydrochloride (12).** Bright yellow solid, yield 95%. $^1$H NMR (DMSO-$d_6$+$D_2O$): $\delta$ 8.80 (s, 1H), 8.42 (d, 2H), 8.20 (d, 2H), 7.68 (t, 2H), 7.60 (t, 2H), 5.22 (s, 2H), 4.20(m, 1H), 3.28 (t, 2H), 3.1∼2.80 (m, 6H), 1.78 (brs, 4H). $^{13}$C NMR ($D_2O$): $\delta$ 130.6, 130.4, 130.0, 129.5, 127.7, 125.5, 122.5, 120.3, 63.8, 50.1, 47.3, 47.2, 42.8, 42.4, 23.0, 22.9. HRMS (FAB): calcd for $C_{22}H_{30}N_3O$ (M + H-3HCl)$^+$: 352.2389; found: 352.2381. Anal. ($C_{22}H_{32}Cl_3N_3O$·0.4$H_2O$) C, H, N.

***N*-{4-[(Anthracen-9-ylmethyl)-amino]-butyl}-cyclohexane-1,4-diamine Trihydrochloride (13) .** Bright yellow solid, yield 95%. $^1$H NMR ($CD_3OD$): $\delta$ 8.68 (s, 1H), 8.41 (d, 2H), 8.17 (d, 2H), 7.68 (t, 2H), 7.57 (t, 2H), 5.34 (s, 2H), 3.40 (m, 2H), 3.16 (m, 4H), 2.26(m, 2H), 2.20(m, 2H), 1.90(m, 4H), 1.60(m, 4H); $^{13}$C NMR($D_2O$): $\delta$ 130.7, 130.4, 130.1, 129.5, 127.7, 125.5, 122.5, 120.3, 55.4, 48.7, 47.1, 44.3, 42.8, 28.2, 26.8, 23.3, 23.0. HRMS (FAB): calcd for $C_{25}H_{34}N_3$ (M + H-3HCl)$^+$: 376.2753; found: 376.2747. Anal. ($C_{25}H_{36}Cl_3N_3$·1.0$H_2O$) C, H, N.

**N$^1$-Anthracen-9-ylmethyl-butane-1,4-diamine Dihydrochloride (14).** Yellow solid; yield 21%; $R_f$ = 0.11, methanol/chloroform, 1:20 + 3 drops of $NH_4OH$); $^1$H NMR (300 MHz, $D_2O$): $\delta$ 8.55 (br s, 1H), 8.15 (d, 2H), 8.08 (d, 2H), 7.66 (m, 4H), 5.08 (br s, 2H), 3.25 (t, 2H), 3.0 (t, 2H), 1.76 (m, 4H); $^{13}$C NMR ($D_2O$): $\delta$ 130.6, 130.3, 129.9, 129.4, 127.6, 125.4, 122.4, 120.2, 47.2, 42.7, 38.6, 24.2, 22.9; ESI-MS *m*/*z* calcd for $C_{19}H_{23}N_2$ (M + H): 279.2; found: 279.2. Anal. ($C_{19}H_{24}N_2Cl_2$,·0.2$H_2O$) C, H, N.

**N$^1$-Anthracen-9-ylmethyl-butylamine monohydrochloride (15)** was synthesized in a previous report.[3]

**(8-Amino-octyl)-carbamic Acid *tert*-butyl Ester (17a).** white solid; yield 78%; $R_f$ = 0.33, methanol/chloroform, 1:9; $^1$H NMR (300 MHz, $CDCl_3$) $\delta$ 4.50 (br s, 1H, BocNH), 3.18 (m, 2H), 2.65 (t, 2H), 1.42 (br s, 12H), 1.36 (br s, 9H); $^{13}$C NMR: $\delta$ 155.7, 78.9, 42.1, 40.5, 33.7, 30.0, 29.3, 29.2, 28.4 (3C), 26.8, 26.7; HRMS (FAB) *m*/*z* calcd for $C_{13}H_{29}N_2O_2$ (M + H)$^+$: 245.2229; found: 245.2235.

**4-(*N*-Benzylamino)-butan-1-ol (19a)**. Pale yellow liquid; yield 89%; $R_f$ = 0.34, methanol/chloroform, 1:4); $^1$H NMR (300 MHz, $CDCl_3$) $\delta$ 7.29 (brs, 5H), 3.77 (s, 2H), 3.59 (t, 2H), 2.68 (t, 2H), 1.65 (brs, 4H); $^{13}$C NMR: $\delta$ 138.8, 128.4 (2C), 128.1 (2C), 127.1, 62.5, 53.7, 49.1, 32.4, 28.5; HRMS (FAB) *m*/*z* calcd for $C_{11}H_{18}NO$(M + H)$^+$: 180.1388; found: 180.1389. Anal. ($C_{11}H_{17}NO$·0.25$H_2O$) C, H, N.

***N*-(Naphthalen-1-ylmethyl)-4-amino-butan-1-ol (19b)**. Dark yellow liquid; yield 93.6%; $R_f$ = 0.54, methanol/chloroform, 1:4); $^1$H NMR (300 MHz, $CDCl_3$) $\delta$ 8.02 (d, 1H), 7.85 (d, 1H), 7.76 (d, 1H), 7.47 (m, 4H), 4.23 (s, 2H), 3.58 (t,

2H), 2.79 (t, 2H), 2.51 (brs, 2H), 1.68 (brs, 4H); $^{13}$C NMR: $\delta$ 134.5, 133.6, 131.3, 128.6, 127.8, 126.2, 126.1, 125.5, 125.2, 122.9, 62.4, 51.0, 49.6, 32.1, 28.3; HRMS *m/z* calcd for $C_{15}H_{19}NO(M^+)$: 229.1467; found: 229.1477. Anal. ($C_{15}H_{19}NO\cdot0.2H_2O$) C, H, N.

**4-[(Anthracen-9-ylmethyl)-amino]-butan-1-ol (19c).**[3] Bright yellow solid; yield 81%; $R_f = 0.51$, methanol/chloroform, 1:9; $^1$H NMR (300 MHz, $CDCl_3$): $\delta$ 8.40 (s, 1H), 8.26 (d, 2H), 8.00 (d, 2H), 7.49 (m, 4H), 4.68 (s, 2H), 3.50 (t, 2H), 2.90 (t, 2H), 1.65 (br s, 4H); $^{13}$C NMR: $\delta$ 131.7, 130.7, 130.5, 129.5, 127.8, 126.6, 125.3, 124.0, 62.9, 50.6, 45.7, 32.7, 29.1. HRMS (FAB) *m/z* calcd for: $C_{19}H_{22}NO$ $(M + H)^+$: 280.1701; found: 280.1679. Anal. ($C_{19}H_{21}NO$) C, H, N.

**4-[(Pyren-1-ylmethyl)-amino]-butan-1-ol (19d).** White solid; yield 94%. $^1$H NMR (300 MHz, $CDCl_3$): $\delta$ 8.24 (d, 2H), 8.13 (m, 4H), 7.96 (m, 4H), 4.42 (s, 2H), 3.56 (t, 2H), 2.82 (t, 2H), 1.64 (brs, 4H). $^{13}$C NMR ($CDCl_3$): 132.4, 131.0, 130.6, 130.5, 128.7, 127.7, 127.2, 127.0 (2C), 125.7, 125.0, 124.9, 124.8, 124.6 (2C), 122.4, 62.6, 51.3, 49.6, 32.3, 28.6. HRMS (FAB): calcd for $C_{21}H_{22}NO(M + H)^+$: 304.1701; found: 304.1701. Anal. ($C_{21}H_{21}NO\cdot0.2H_2O$) C, H, N.

**Acknowledgment.** This work was supported in part by the Elsa U. Pardee Foundation and the Florida Hospital Gala Endowed Program for Oncologic Research. The authors wish to thank the Chinese Scholarship Council for partial support of C.W.

## References

(1) Phanstiel, O., IV; Price, H. L,; Wang, L.; Juusola, J.; Kline, M.; Shah, S. M. The Effect of Polyamine Homologation on the Transport and Cytotoxicity Properties of Polyamine-(DNA-Intercalator) Conjugates. *J. Org. Chem*. **2000**, *65*, 5590−5599.

(2) Wang, L.; Price, H. L.; Juusola, J.; Kline, M.; Phanstiel, IV, O. The Influence of Polyamine Architecture on the Transport and Topoisomerase II Inhibitory Properties of Polyamine DNA-Intercalator Conjugates. *J. Med. Chem*. **2001**, *44*, 3682−3691.

(3) Wang, C.; Delcros, J.-G.; Biggerstaff, J.; Phanstiel IV, O. Synthesis and Biological Evaluation of $N^1$-(anthracen-9-ylmethyl)-triamines as Molecular Recognition Elements for the Polyamine Transporter. *J. Med. Chem*. **2003**, *46*, 2663−2671.

(4) Wang, C.; Delcros, J.-G.; Biggerstaff, J.; Phanstiel IV, O. Molecular Requirements for Targeting the Polyamine Transport System: Synthesis and Biological Evaluation of Polyamine-Anthracene Conjugates. *J. Med. Chem*. **2003**, *46*, 2672−2682.

(5) Bergeron, R. J.; Feng, Y.; Weimar, W. R.; McManis, J. S.; Dimova, H.; Porter, Carl; Raisler, B.; Phanstiel, O. A Comparison of Structure−Activity Relationships between Spermidine and Spermine Analogue Antineoplastics. *J. Med. Chem*. **1997**, *40*, 1475−1494.

(6) (a) Cullis, P. M.; Green, R. E.; Merson-Davies, L.; Travis, N. Probing the mechanism of transport and compartmentalisation of polyamines in mammalian cells. *Chem. Biol*. **1999**, *6*, 717−729 and refs therein. (b) Seiler, N.; Dezeure, F. Polyamine transport in mammalian cells. *Int. J. Biochem*. **1990**, *22*, 211−218. (c) Seiler, N.; Delcros J−G.; Moulinoux, J. P. Polyamine Transport in Mammalian Cells. An Update. *Int. J. Biochem. Cell. Biol*. **1996**, *28*, 843−861.

(7) Kramer, D. L.; Miller, J. T.; Bergeron, R. J.; Khomutov, R.; Khomutov, A.; Porter, C. W. Regulation of polyamine transport by polyamines and polyamine analogues. *J. Cell. Physiol*. **1993**, *155*, 399−407.

(8) Sugiyama, S.; Matsuo, Y.; Maenaka, K.; Vassylyev, D. G.; Matsushima, M.; Kashiwagi, K.; Igarashi, K.; Morikawa, K. The 1.8-A X-ray structure of the *Escherichia coli* PotD protein complexed with spermidine and the mechanism of polyamine binding. *Protein Sci*. **1996**, *5*, 1984−1990.

(9) Vassylyev, D. G.; Tomitori, H.; Kashiwagi, K.; Morikawa, K.; Igarashi, K. Crystal structure and mutational analysis of the *Escherichia coli* putrescine receptor. Structural basis for substrate specificity. *J. Biol. Chem*. **1998**, *273*, 17604−17609.

(10) Kashiwagi, K.; Endo, H.; Kobayashi, H.; Takio, K.; Igarashi, K. Spermidine-preferential uptake system in *Escherichia coli*. ATP hydrolysis by PotA protein and its association with membrane. *J. Biol. Chem*. **1995**, *270*, 25377−25382.

(11) Kashiwagi, K.; Miyamoto, S.; Nukui, E.; Kobayashi, H.; Igarashi, K. Functions of potA and potD proteins in spermidine-preferential uptake system in *Escherichia coli*. *J. Biol. Chem*. **1993**, *268*, 19358−19363.

(12) Tomitori, H.; Kashiwagi, K.; Sakata, K.; Kakinuma, Y.; Igarashi, K. Identification of a gene for a polyamine transport protein in yeast. *J. Biol. Chem*. **1999**, *274*, 3265−3267.

(13) (a) Bergeron, R. J.; Wiegand, J.; McManis, J. S.; Weimar, W. R.; Smith, R. E.; Algee, S. E.; Fannin, T. L.; Slusher, M. A.; Snyder, P. S. Polyamine Analogue Antidiarrheals: A Structure−Activity Study. *J. Med. Chem*. **2001**, *44*, 232−244. (b) Bergeron, R. J.; Yao, G. W.; Yao, H.; Weimar, W. R.; Sninsky, C. A.; Raisler, B.; Feng, Y.; Wu, Q.; Gao, F. "Metabolically Programmed Polyamine Analogue Antidiarrheals. *J. Med. Chem*. **1996**, *39*, 2461−2471. (c) Bergeron, R. J.; Neims, A. H.; McManis, J. S.; Hawthorne, T. R.; Vinson, J. R. T.; Bortell, R.; Ingeno, M. J. Synthetic polyamine analogues as antineoplastics. *J. Med. Chem*. **1988**, *31*, 1183−1190. (d) Casero, R. A., Jr.; Woster, P. M. Terminally Alkylated Polyamine Analogues as Chemotherapeutic Agents. *J. Med. Chem*. **2001**, *44*, 1−26 and references therein.

(14) Delcros, J.-G.; Tomasi, S.; Carrington, S.; Martin, B.; Renault, J.; Blagbrough, I. S.; Uriac, P. Effect of spermine conjugation on the cytotoxicity and cellular transport of acridine. *J. Med. Chem*. **2002**, *45*, 5098−5111.

(15) Azzam, T.; Eliyahu, H.; Shapira, L.; Linial, M.; Barenholz, Y.; Domb, A. J. Polysaccharide-Oligoamine Based Conjugates for Gene Delivery. *J. Med. Chem*. **2002**, *45*, 1817−1824.

(16) Stark, P. A.; Thrall, B. D. Meadows, G. G.; Abdul-Monem, M. M. Synthesis and Evaluation of novel spermidine derivatives as targeted cancer chemotherapeutic agents. *J. Med. Chem*. **1992**, *35*, 4264−4269.

(17) Cohen, G. M.; Cullis, P.; Hartley, J. A.; Mather, A. Symons, M. C. R.; Wheelhouse, R. T. Targeting of Cytotoxic Agents by Polyamines: Synthesis of a Chloroambucil-Spermidine Conjugate. *J. Chem. Soc., Chem. Commun*. **1992**, 298−300.

(18) Cai, J.; Soloway, A. H. Synthesis of Carboranyl Polyamines for DNA Targeting. *Tetrahedron Lett*. **1996**, *37*, 9283−9286.

(19) Ghaneolhosseini, H.; Tjarks, W.; Sjoberg, S. Synthesis of Novel Boronated Acridines and Spermidines as Possible Agents for BNCT. *Tetrahedron* **1998**, *54*, 3877−3884.

(20) Blagbrough, I. S.; Geall, A. J. Homologation of Polyamines in the Synthesis of Lipo-Spermine Conjugates and Related Lipoplexes. *Tetrahedron Lett.* **1998**, 443−446.

(21) Cullis, P. M.; Merson-Davies, L.; Weaver, R. Conjugation of a polyamine to the bifunctional alkylating agent chlorambucil does not alter the preferred cross-linking site in duplex DNA. *J. Am. Chem. Soc.* **1995**, *117*, 8033−8034.

(22) Aziz, S. M.; Yatin, M.; Worthen, D. R.; Lipke, D. W.; Crooks, P. A. A novel technique for visualising the intracellular localization and distribution of transported polyamines in cultured pulmonary artery smooth muscle cells. *J. Pharm. Biomed. Anal*. **1998**, *17*, 307−320.

(23) Saab, N. H.; West, E. E.; Bieszk, N. C.; Preuss, C. V.; Mank, A. R.; Casero, R. A.; Woster, P. M. Synthesis and Evaluation of Polyamine Analogues as Inhibitors of Spermidine/Spermine-$N^1$-Acetyltransferase (SSAT) and as Potential Antitumor agents. *J. Med. Chem*. **1993**, *36*, 2998−3004.

(24) Porter, C. W.; Cavanaugh, P. F.; Ganis, B.; Kelly, E.; Bergeron, R. J. Biological properties of N-4 and N-1, N-8-spermidine derivatives in cultured L1210 leukemia cells. *Cancer Res.* **1985**, *45*, 2050−2057.

(25) Bergeron, R. J.; McManis, J. S.; Weimar, W. R.; Schreier, K. M.; Gao, F.; Wu, Q.; Ortiz-Ocasio, J.; Luchetta, G. R.; Porter, C.; Vinson, J. R. T. The role of charge in polyamine analogue recognition. *J. Med. Chem*. **1995**, *38*, 2278−2285.

(26) Porter, C.; Miller, J.; Bergeron, R. J. Aliphatic chain-length specificity of the polyamine transport system in ascites L1210 leukemia cells. *Cancer Res.* **1984**, *44*, 126−128.

(27) Xia, C. Q.; Yang, J. J.; Ren, S.; Lien, E. J. QSAR analysis of polyamine transport inhibitors in L1210 cells. *J. Drug Targ.* **1998**, *6*, 65−77.

(28) O'Sullivan, M. C.; Golding, B. T.; Smith, L. L. and Wyatt, I. Molecular features necessary for the uptake of diamines and related compounds by the polyamine receptor of rat lung slices. *Biochem. Pharm*. **1991**, *41*, 1839−1848.

(29) Bergeron, R. J.; McManis, J. S.; Liu, C. Z.; Feng, Y.; Weimar, W. R.; Luchetta, G. R.; Wu, Q.; Ortiz-Ocasio, J.; Vinson, J. R. T.; Kramer, D.; Porter, C. "Antiproliferative Properties of Polyamine Analogues: A Structure−Activity Study" *J. Med. Chem*. **1994**, *37*, 4−3476.

(30) Soulet, D.; Covassin, L.; Kaouass, M.; Charest-Gaudreault, R.; Audette, M.; Poulin, R. Role of endocytosis in the internalisation of spermidine-C2−BODIPY, a highly fluorescent probe of polyamine transport. *Biochemical J*. **2002**, *367*, 347−357.

(31) Burns, M. R.; Carlson, C. L.; Vanderwerf, S. M.; Ziemer, J. R.; Weeks, R. S.; Cai, F.; Webb, H. K.; Graminski, G. F. Amino Acid/Spermine Conjugates: Polyamine Amides as Potent Spermidine Uptake Inhibitors. *J. Med. Chem*. **2001**, *44*, 3632−3644.

(32) Mandel, J. L.; Flintoff, W. F. Isolation of mutant mammalian cells altered in polyamine transport. *J. Cell. Physiol*. **1978**, *97*, 335−344.

(33) Byers, T. L.; Wechter, R.; Nuttall, M. E.; Pegg, A. E. Expression of a human gene for polyamine transport in chinese hamster ovary cells. *Biochem. J*. **1989**, *263*, 745−752.

(34) (a) Chaney, S. E.; Kobayashi, K,.; Goto, R.; Digenis, G. A. Tumor selective enhancement of radioactivity uptake in mice treated with α-difluoromethylornithine prior to administration of $^{14}$C-putrescine. *Life Sci*. **1983**, *32*, 1237−1241.(b) Heston, W. D. W.; Kadmon, D.; Covey, D. F.; Fair, W. R. Differential effect of α-difluoromethylornithine on the in vivo uptake of $^{14}$C-labeled polyamines and methylglyoxal bis(guanylhydrazone) by a rat prostate-derived tumor. *Cancer Res.* **1984**, *44*, 1034−1040.(c) Redgate, E. S.; Grudziak, A. G.; Deutsch, M.; Boggs, S. S. Difluoromethylornithine enhanced uptake of tritiated putrescine in 9L rat brain tumors. *Int. J. Radiat. Oncol. Biol. Phys.* **1997**, *38*, 169−174.

(35) Porter, C. W.; Ganis, B.; Vinson, T.; Marton, L. J.; Kramer, D. L.; Bergeron, R. J. Comparison and characterization of growth inhibition in L1210 cells by alpha-difluoromethylornithine, an inhibitor of ornithine decarboxylase, and N1, N8-bis(ethyl)-spermidine, an apparent regulator of the enzyme. *Cancer Res.* **1986**, *46*, 6279−6285.

(36) (a) Kumar, C. V.; Asuncion, E. H. DNA Binding Studies and Site Selective Fluorescence Sensitization of an Anthryl Probe. *J. Am. Chem. Soc.* **1993**, *115*, 8547−8553. (b) Rodger, A.; Taylor, S.; Adlam, G.; Blagbrough, I. S.; Haworth, I. S. Multiple DNA Binding Modes of Anthracene-9-Carbonyl-*N*$^1$-Spermine. *Bioorg. Med. Chem*. **1995**, *3*, 861−872.

(37) Wang, C.; Abboud, K. A.; Phanstiel, O. IV Synthesis and Characterization of N1-(4-toluenesulfonyl)-N1-(9-anthracenemethyl)triamines. *J. Org. Chem*. **2002**, *67*, 7865−7868.

(38) Blagbrough, I. S.; Geall, A. J. Practical Synthesis of Unsymmetrical Polyamine Amides. *Tetrahedron Lett.* **1998**, 439−442.

(39) Kuksa, V.; Buchan, R.; Lin, P. K. T. Synthesis of Polyamines, Their Derivatives, Analogues and Conjugates. *Synthesis* **2000**, No. 9, 1189−1207.

(40) (a) Pegg, A. E. The role of polyamine depletion and accumulation of decarboxylated S-adenosylmethionine in the inhibition of growth of SV-3T3 cells treated with alpha-difluoromethylornithine. *Biochem. J*. **1984**, *224*, No. 1, 29−38. (b) Seiler, N.; Knödgen, B. Determination of polyamines and related compounds by reversed-phase high-performance liquid chromatography: Improved separation systems. *J. Chromatography* **1985**, *339*, 45−57. (c) Gaboriau, F.; Havouis, R.; Moulinoux, J.-P.; Delcros, J.-G. Atmospheric pressure chemical ionization-mass spectrometry method to improve the determination of dansylated polyamines. *Anal. Biochem*. **2003**, *318*, 212−220. (d) Martin, B.; Possémé, F.; Le Barbier, C.; Carreaux, F.; Carboni, B.; Seiler, N.; Moulinoux, J.-P.; Delcros, J.-G. N−Benzylpolyamines as Vectors of Boron and Fluorine for Cancer Therapy and Imaging: Synthesis and Biological Evaluation. *J. Med. Chem*. **2001**, *44*, 3653−3664.

(41) Cheng, Y.-C.; Prusoff, W. H. Relationship between the inhibition constant (Ki) and the concentration of inhibitor which causes 50% inhibition (IC50) of an enzymatic reaction. *Biochem. Pharmacol.* **1973**, *22*, 3099−3108.

(42) Bergeron, R. J.; Müller, R.; Bussenius, J.; McManis, J. S.; Merriman, R. L.; Smith, R. E.; Yao, H.; Weimar, W. R. Synthesis and Evaluation of Hydroxylated Polyamine Analogues as Antiproliferatives. *J. Med. Chem*. **2000**, *43*, 224−235.

(43) Covassin. L.; Desjardins, M.; Charest-Gaudreault, R.; Audette, M.; Bonneau, M. J.; Poulin, R. Synthesis of spermidine and norspermidine dimers as high affinity polyamine transport inhibitors. *Bioorg. Med. Chem. Lett.* **1999**, *9*, 1709−1714.

(44) (a) Fransson, L.-A. Glypicans. *Int. J. Biochem. Cell Biol.* **2002**, *1348*, 1−5. (b) Belting, M.; Borsig, L.; Fuster, M. M.; Brown, J. R.; Persson, L.; Fransson, L.-A.; Esko, J. D. Tumor attenuation by combined heparan sulfate and polyamine depletion. *Proc. Natl. Acad. Sci. U.S.A.* **2002**, *99*, 371−376. (c) Belting, M.; Persson, S.; Fransson, L.-A. Proteoglycan involvement in polyamine uptake. *Biochem. J.* **1999**, *338*, 317−323.

(45) Mislick, K. A.; Baldeschwieler, J. D. Evidence for the role of proteoglycans in cation-mediated gene transfer. *Proc. Natl. Acad. Sci. U.S.A.* **1996**, *93*, 12349−12354.

(46) Mounkes, L. C.; Zhong, W.; Cipres-Palacin, G.; Heath, T. D.; Debs, R. J. Proteoglycans Mediate Cationic Liposome-DNA Complex-based Gene Delivery in Vitro and in Vivo. *J. Biol. Chem*. **1998**, *273*, 26164−26170.

(47) Mosmann, T. Rapid colorimetric assay for cellular growth and survival: application to proliferation and cytotoxicity assays. *J. Immunol. Methods* **1983**, *65*, 55−63.

(48) Clément, S.; Delcros, J. G.; Feuerstein, B. G. Spermine uptake is necessary to induce haemoglobin synthesis in murine erythroleukemia cells. *Biochem. J*. **1995**, *312*, 933−938.

(49) Torossian, K.; Audette, M.; Poulin, R. Substrate protection against inactivation of the mammalian polyamine transport system by 1-ethyl-3-(3-dimethylaminopropyl)-carbodiimide. *Biochem. J*. **1996**, *319*, 21−26.

JM030223A